XII CONGRESSO DE CONSTRUÇÃO METÁLICA E MISTA

TEMA ESPECIAL

ESTRUTURAS METÁLICAS COMO RESPOSTA ÀS ALTERAÇÕES CLIMÁTICAS

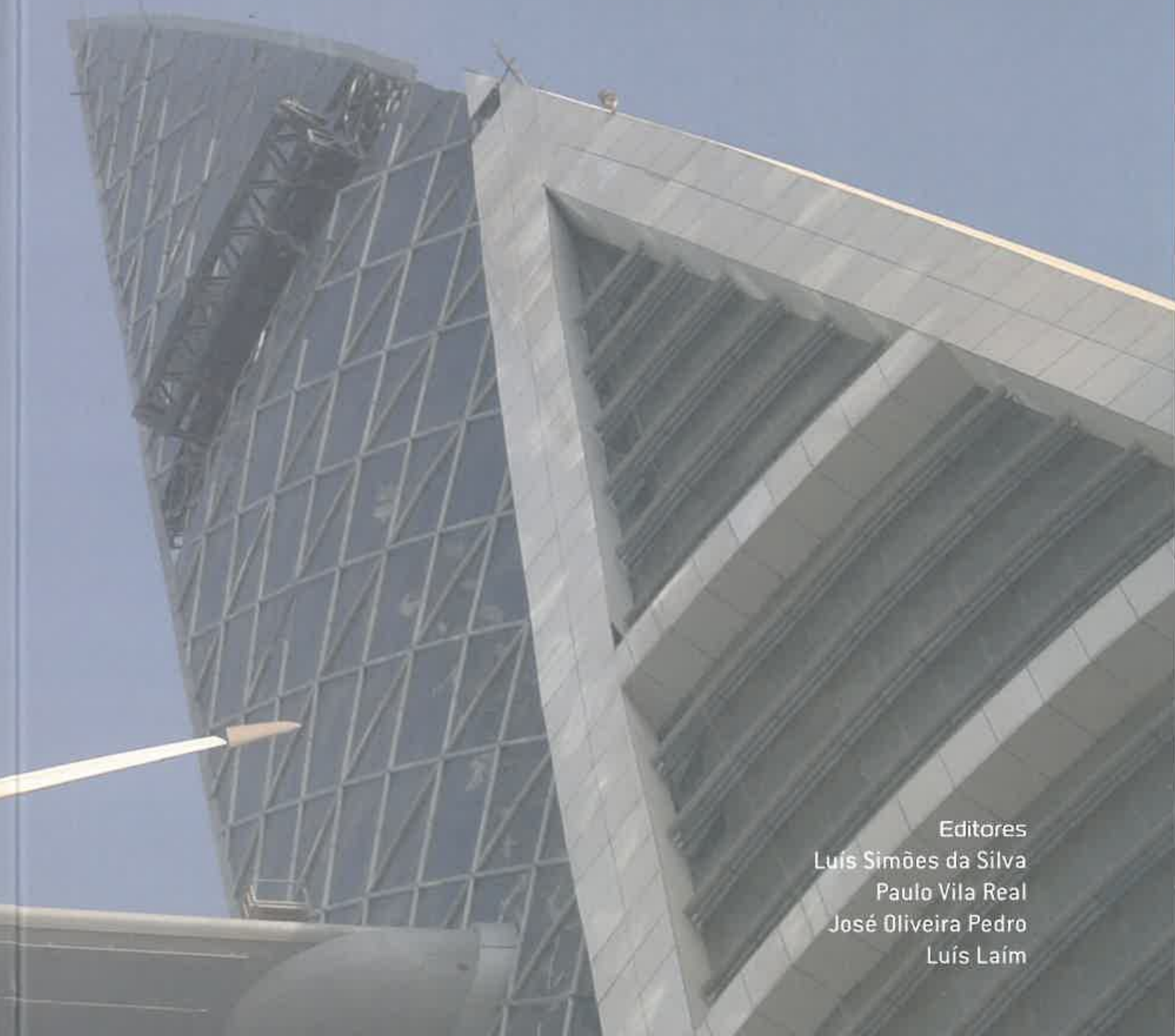

Editores
Luís Simões da Silva
Paulo Vila Real
José Oliveira Pedro
Luís Laím

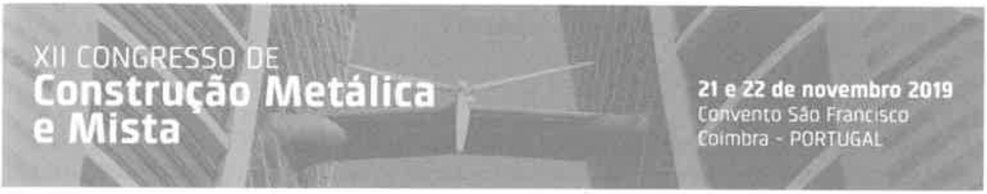

Atas do XII Congresso de Construção Metálica e Mista

Coimbra
21 e 22 de novembro de 2019

Luís Simões da Silva

Departamento de Engenharia Civil
Faculdade de Ciências e Tecnologia da Universidade de Coimbra
Coimbra, Portugal

Paulo Vila Real

Departamento de Engenharia Civil
Universidade de Aveiro
Aveiro, Portugal

José Oliveira Pedro

Departamento de Engenharia Civil, Arquitectura e Georrecursos
Instituto Superior Técnico da Universidade de Lisboa
Lisboa, Portugal

Luís Laím

Departamento de Engenharia Civil
Faculdade de Ciências e Tecnologia da Universidade de Coimbra
Coimbra, Portugal

organização: **CMM** – Associação Portuguesa de Construção Metálica e Mista

cmm
ASSOCIAÇÃO PORTUGUESA DE CONSTRUÇÃO METÁLICA E MISTA

XII Congresso de Construção Metálica e Mista

Editora:

cmm – Associação Portuguesa de Construção Metálica e Mista
Business Center Leonardo da Vinci
Coimbra iParque Lote 3
3040-540 Coimbra, Portugal
Tel.: +351 239 098 422; Tlm.: +351 965 061 249; Fax: +351 239 091 216
Email: cmm@cmm.pt
Url: www.cmm.pt

1ª Edição: Novembro 2019

Tiragem: 350 exemplares

Depósito legal: 463463/19
ISBN: 978-989-99251-6-8

Coordenação editorial: Luís Figueiredo Silva
Conceção gráfica da capa: 3LM
Formatação de conteúdos e paginação: Ana Valente
Impressão: Sersilito, Empresa Gráfica Lda., Maia, Portugal

Nota da editora

Este texto foi elaborado a partir da reprodução dos originais preparados pelos autores. Por conseguinte, a editora não pode aceitar qualquer responsabilidade pelo conteúdo, nem por possíveis erros no texto.

Prefácio

O XII Congresso de Construção Metálica e Mista realiza-se num período em que o setor da Construção Metálica portuguesa se continua a afirmar como um motor de inovação e de internacionalização da indústria nacional. Com um volume de negócios superior a 4,5 mil milhões de euros (2018) e um volume de exportações de cerca de 3,1% das exportações do país, podemos assegurar que presentemente este setor possui uma grande vitalidade, é tecnologicamente avançado e é detentor de uma forte capacidade competitiva internacional.

A CMM mantém, assim, a sua aposta na inovação tecnológica e a competitividade do setor, pretendendo potenciar uma plataforma de conciliação entre todos os atores do setor, em torno de uma estratégia e programa de ação definido para a consolidação do setor, com o foco no mercado global e potenciando o reconhecimento de excelência que detêm, contribuindo de forma decisiva para a afirmação da Construção Metálica Portuguesa a nível mundial, como uma solução construtiva sustentável de alta qualidade e inovadora.

O XII Congresso de Construção Metálica e Mista é a maior e mais relevante conferência nacional de construção metálica e mista, com realização bienal e promovido pela CMM, e reúne projetistas, empresas do sector e investigadores, contando com a participação de conferencistas nacionais e internacionais de renome. No seguimento das edições anteriores o XII Congresso de Construção Metálica e Mista volta a apostar na promoção do uso de materiais de matriz metálica e mista na construção e assumir uma posição ativa da promoção da inovação no setor da construção metálica a nível nacional e internacional, bem como, difundir as mais recentes inovações no âmbito deste tipo de construção e dar a conhecer as linhas de orientação da investigação neste campo, fomentando o intercâmbio de experiências.

À semelhança das onze edições anteriores, o XII Congresso de Construção Metálica e Mista será composto por Sessão de Palestras e Sessões Científicas e Técnicas, por Workshops e apresentações técnico-comerciais das empresas presentes, bem como uma Exposição Técnica, que conta com várias empresas e entidades relevantes do setor, sendo este um espaço privilegiado para a troca de experiências entre as empresas e os técnicos do setor. Nesta edição serão também promovidas reuniões B2B entre empresas participantes no evento, reforçando também a componente comercial entre as empresas deste setor.

A décima segunda edição do Congresso de Construção Metálica e Mista, é dedicada ao tema "Estruturas metálicas como resposta às alterações climáticas", sensibilizando os técnicos da fileira da construção metálica para a importância deste tema, bem como os desafios da digitalização e industrialização, vulgarmente denominados de "Indústria 4.0".

Luís Simões da Silva
Presidente da CMM e da Comissão Organizadora do
XII Congresso de Construção Metálica e Mista

Comissão Organizadora

Luís Simões da Silva, CMM
José Oliveira Pedro, IST
Luís Laím, UC

Comissão Científica

Paulo Vila Real, UA
Abílio de Jesus, FEUP
Aldina Santiago, UC
Alexandra Feliz, O FELIZ
Alfredo Dias, UC
Altino Loureiro, UC
António Adão da Fonseca, FEUP
António Baptista, LNEC
António Matos Silva, MARTIFER SA
António Reis, IST
Bruno Marques, FERPINTA
Carlos Couto, UA
Carlos Martins, MARTIFER SA
Carlos Poço, O POÇO SA
Carlos Rebelo, UC
Constança Rigueiro, UC
Dinar Camotim, IST
Diogo Ribeiro, ISEP
Dulce Rodrigues, UC
Elsa Caetano, FEUP
Filipe Santos, VESAM Group
Francisco Virtuoso, IST
Helena Gervásio, UC
Isabel Valente, UM
Humberto Varum, FEUP
João Almeida Fernandes, LNEC
João Paulo Rodrigues, UC
João Pedro Martins, UC
João Rocha de Almeida, UNL
Jorge Paiva, CIN
José António Correia, INEGI
José Clemente, REFER
José Miguel Castro, FEUP
José Oliveira Pedro, IST
Leonor Côrte-Real, HEMPEL
Luís Borges, STRUCTURAME
Luís Bragança, UM
Luís Calado, IST
Luís Câncio, J.L. CÂNCIO MARTINS, LDA
Luís Godinho, UC
Luís Laím, UC
Luís Simões da Silva, UC
Manuela Salta, LNEC
Nuno Lopes, UA
Nuno Silvestre, IST
Paulo Piloto, IPB
Paulo Santos, UC
Rodrigo Gonçalves, UNL
Rui Alves, PROINDUSTRIAL
Rui Calçada, FEUP
Rui Simões, UC
Sandra Jordão, UC
Tiago Abecasis, TAL PROJECTO, Lda.
Tiago Mendonça, BETAR
Victor Ferreira, UA
Vítor Murtinho, UC

Comissão Executiva

Luís Figueiredo Silva, CMM
Ana Valente, CMM
Joana Albuquerque, CMM
Zínia Antunes, CMM

Índice

Pontes Metálicas e Mistas

Segurança Estrutural e Desempenho de Novos Materiais e Produtos

Soluções Industrializadas para a Construção de Edifícios

Índice de Autores

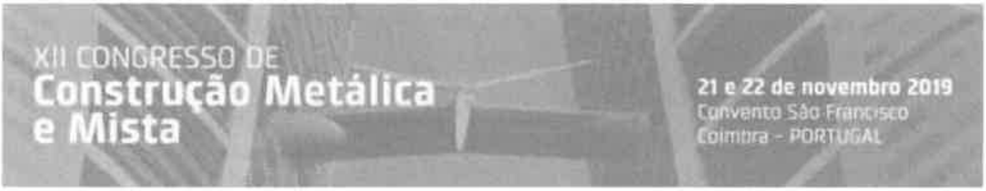

IMPROVED CALCULATION METHODS FOR THE TEMPERATURE OF THE STEEL COMPONENTS OF COMPOSITE SLABS UNDER FIRE CONDITIONS

Paulo A. G. Piloto[a*], Carlos Balsa[b], Fernando F. Ribeiro[c] and Ronaldo Rigobello[d]

[a,b] *Polytechnic Institute of Bragança – IPB*
[c,d] *Federal University of Technology - Paraná – UTFPR*

[*] Author for contact. Tel.: +351 273 303 037; E-mail: ppiloto@ipb.pt

Abstract. A composite steel-concrete slab consists of a profiled steel deck that acts as permanent formwork to the concrete topping, which is normally reinforced with individual rebars and an anti-crack mesh. The Annex D of the EN 1994-1-2 provides guidelines for the calculation of the temperature of the rebars and the parts of the steel deck of composite slabs subjected to the standard fire from below. However, no revisions were made to these methods during the last two decades. This work proposes an improved method for the estimation of the temperature of the parts of the steel deck and the rebars as well. The proposed expressions are derived from numerical simulations using a 3-D finite element model, considering perfect thermal contact between all the materials.

1. Introduction

A composite steel-concrete slab consists of a concrete topping cast on the top of a profiled steel deck. Normally, the concrete is reinforced with an anti-crack mesh positioned on the upper part and individual reinforcing bars placed within the ribs, see Fig. 1. This type of slab is broadly used in buildings due to its several advantages, such as the reduction or elimination of propping and the simplicity of installation.

The use of composite slabs in buildings has become very popular since the decade of 1980. The most popular types of shapes of the profiled steel deck are trapezoidal and re-entrant. Slabs with trapezoidal steel deck are more popular than re-entrant ones owing to the ease of casting concrete. The overall thickness of composite slabs usually varies between 100 and 170 mm, and the steel deck thickness between 0.7 and 1.2 mm.

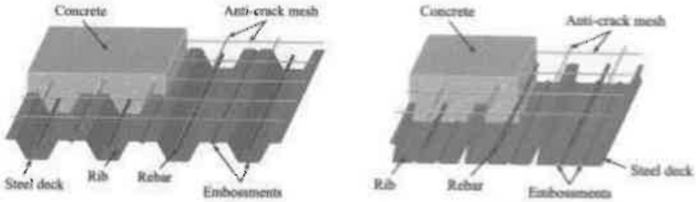

a) Trapezoidal profile b) Re-entrant profile
Fig. 1: Typical layout of composite slabs

Composite slabs need to meet fire-safety requirements in accordance to standards and regulations. Usually, this structural element is fire rated on the basis of standard fire tests, using the standard fire curve ISO 834 [1]. The fire resistance of composite slabs should be determined according to three different criteria, namely load bearing (R), integrity (E) and thermal insulation (I).

The profiled geometry of the steel deck and the existence of the ribs in composite slabs creates an orthotropic profile, resulting in complex thermal gradients, hence representing challenges in numerical modelling [2]. In recent years, several investigations have been carried out in order to analyse the fire behaviour of this structural element.

In 1983, recognizing the need for a calculation method, the ECCS (European Convention for Constructional Steelwork) [3] published the first recommendations for the practical design of composite slabs under fire conditions. This technical note introduced simple calculation methods based on criteria for fire resistance of the standard ISO 834, hence inspiring the diffusion of the use of composite slabs.

In 1991, Hamerlinck [4] conducted a numerical and experimental investigation concerning the thermal and mechanical behaviour of composite slabs under fire conditions. Both numerical models were experimentally validated with loaded and unloaded tests. It was observed that the developed two-dimensional model provided satisfactory results on the thermal behaviour of composite slabs although not including three-dimensional thermal effects.

In 1998, Both [5] performed a numerical and experimental study with the main objective of introducing easy to handle calculation rules as well as providing more insight on the fire behaviour and failure mechanisms mainly of continuous composite slabs. A parametric study was performed and simple calculation rules were derived from the results using standard regression techniques. It was concluded that the thermal model was able to describe the two and three-dimensional heat flow in composite slabs during fire exposure and the assessment rules for the fire resistance given in the Eurocode 4 at that time could be considerably improved, among other conclusions.

In 2002, Lim and Wade [6] performed fire tests on six large-scale concrete slabs, comprising three reinforced concrete flat slabs and three composite steel-concrete slabs. The main objective of the tests was to analyse the fire behaviour of unrestrained simply supported slabs in a controlled furnace. In general, the measured fire resistance was higher than the predictions from normative recommendations. The results evidenced the important effect of membrane action on preserving the structural stability of the slabs under fire conditions.

In 2011, Guo and Bailey [7] conducted an experimental study with the objective of providing more insight on the behaviour of composite slabs during heating and cooling phases of fire. The specimens were loaded with representative values found in practice to investigate the structural behaviour. For all the tests, the maximum temperatures on the unexposed surface and on the mesh were both higher during the cooling stages, due to the thermal inertial effect.

In 2019, Jian Jiang et al. [2] carried out a numerical investigation around different parameters that may influence on the fire resistance of composite slabs with respect to the thermal insulation criterion (I). An improved algebraic expression for the calculation of the fire resistance that explicitly accounts for moisture content of concrete was proposed. A set of 54 composite slabs was selected for numerical analyses using a high-fidelity finite element approach. It was concluded that the concrete thickness and the moisture content were the parameters that most influenced the fire resistance.

The scope of this study concerns three-dimensional numerical simulations using the standard fire curve ISO 834 [1] in order to evaluate the temperature of the steel components of composite slabs. A thermal model considering perfect thermal contact between the materials is implemented using ANSYS Mechanical APDL. The numerical model is validated against experimental results published by Hamerlinck [4], and the results are compared to the simplified calculation method of Eurocode 4 – Part 1-2. Thereafter, a parametric study comprising different steel deck profiles is conducted, and new calculation methods are presented for the temperatures of the parts of the steel deck and the rebars.

2. Simplified calculation method of Eurocode 4

The annex D of EN 1994-1-2 [8] presents a simplified calculation method for the determination of the temperature of the parts of the steel deck and the rebars of composite slabs subjected to the standard fire curve ISO 834 from below. These temperatures are important for the calculation of the sagging moment resistance and the fire resistance according to the load bearing criterion (R). The temperatures of the parts of the steel deck θ_a (°C) should be calculated according to Eq. (1).

$$\theta_a = b_0 + b_1 \cdot 1/l_3 + b_2 \cdot A/L_r + b_3 \cdot \Phi_{up} + b_4 \cdot \Phi_{up}^2 \quad (1)$$

In the equation above, l_3 is the width of the upper flange (mm), A/L_r is the rib geometry factor (mm), and Φ_{up} is the view factor of the upper flange (dimensionless). The partial factors b_i are coefficients that differ for slabs with normal weight concrete (NWC) and lightweight concrete. Table 1 presents these coefficients for each part of the steel deck for slabs with NWC.

The rib geometry factor can be calculated using the geometric parameters of the slab, as follows.

$$A/L_r = h_2 \cdot \left((l_1 + l_2)/2\right) \Big/ \left(l_2 + 2\sqrt{h_2^2 + \left((l_1 - l_2)/2\right)^2}\right) \quad (2)$$

Table 1: Coeff. for the deter. of the temp. of the parts of the steel deck for slabs with NWC ([8])

Standard fire resistance	Part of the steel deck	b_0 (°C)	b_1 (°C mm)	b_2 (°C mm)	b_3 (°C)	b_4 (°C)
R60	Lower flange	951	-1197	-2.32	86.4	-150.7
	Web	661	-833	-2.96	537.7	-351.9
	Upper flange	340	-3269	-2.62	1148.4	-679.8
R90	Lower flange	1018	-839	-1.55	65.1	-108.1
	Web	816	-959	-2.21	464.9	-340.2
	Upper flange	618	-2786	-1.79	767.9	-472.0
R120	Lower flange	1063	-679	-1.13	46.7	-82.8
	Web	925	-949	-1.82	344.2	-267.4
	Upper flange	770	-2460	-1.67	592.6	-379.0

The temperature of the rebars in the rib θ_s (°C) shall be determined according to Eq. (3).

$$\theta_s = c_0 + (c_1 \cdot u_3/h_2) + (c_2 \cdot z) + (c_3 \cdot A/L_r) + (c_4 \cdot \alpha) + (c_5 \cdot 1/l_3) \quad (3)$$

In the equation above, u_3 is the distance of the rebar to the lower flange (mm); h_2 is the thickness of the concrete part (mm); z is an indication of the position in the rib ($mm^{-0.5}$); and α is the angle of the web (degrees). The partial factors c_i depend on the fire resistance (R) and differ for slabs with NWC and lightweight concrete. Table 2 gives these coefficients for slabs with NWC.

Table 2: Coefficients for the determination of the temperatures of the rebars in the rib for slabs with NWC (adapted from EN 1994-1-2 [8])

Standard fire resistance	c_0 (°C)	c_1 (°C)	c_2 (°C $mm^{0.5}$)	c_3 (°C mm)	c_4 (°C/°)	c_5 (°C mm)
R60	1191	-250	-240	-5.01	1.04	-925
R90	1342	-256	-235	-5.30	1.39	-1267
R120	1387	-238	-227	-4.79	1.68	-1326

The z-factor should be calculated according to the following equation.

$$1/z = 1/\sqrt{u_1} + 1/\sqrt{u_2} + 1/\sqrt{u_3} \tag{4}$$

In the equation above, u_1 and u_2 are defined as the shortest distances of the centre of the rebar to any point of the webs of the steel deck (mm); and u_3 is the distance of the centre of the rebar to the lower flange of the steel deck (mm).

The simplified calculation method also provides general rules for the determination of the load bearing capacity of composite steel-concrete slabs. Based on a global plastic analysis, the design for bending resistance should be determined using Eq. (5).

$$M_{fi,t,Rd} = \sum_{i=1}^{n=4} A_i \cdot z_i \cdot k_{y,\theta,i} \cdot \left(\frac{f_{y,i}}{\gamma_{M,fi}} \right) + \alpha_{slab} \cdot \sum_{j=1}^{m=1} A_j \cdot z_j \cdot k_{c,\theta,j} \cdot \left(\frac{f_{c,j}}{\gamma_{M,fi,c}} \right) \tag{5}$$

The coordinates z_i and z_j are the distances of the components for steel and concrete materials, between the geometric centre and the neutral axis of the slab under fire conditions. The coefficients $k_{y,\theta,i}$ and $k_{c,\theta,i}$ represent the reduction coefficients for the yielding stress of steel and the compressive strength of concrete, affected by the temperature of each component, being defined by standards for steel [9] and concrete [10]. The coefficient $k_{y,\theta,i}$ may have different values, according to the type of steel (cold-formed carbon steel for the design of class 4 sections at elevated temperatures [8] and cold-formed carbon steel for rebars [9]). The model assumes no reduction for concrete.

The neutral axis under fire conditions can be defined by the equilibrium of Eq. (6) [8]. This axis modifies its position during fire, moving from the hot region to the cold region, assuming different positions for R60, R90 and R120.

$$\sum_{i=1}^{n=4} A_i \cdot k_{y,\theta,i} \cdot \left(\frac{f_{y,i}}{\gamma_{M,fi}} \right) + \alpha_{slab} \cdot \sum_{j=1}^{m=1} A_j \cdot k_{c,\theta,j} \cdot \left(\frac{f_{c,j}}{\gamma_{M,fi,c}} \right) = 0 \tag{6}$$

The analytical expressions given in the current version of this standard are based on the study conducted by Both [5] in 1998. During the last years, no revisions were made to this method [2].

3. Experimental fire test

The experimental fire test conducted by Hamerlinck [4] (test number 2) has been selected for the validation of the numerical thermal model. The simply supported slab was exposed to the ISO 834 standard fire from bellow in a controlled furnace. The profile of the composite slab is illustrated in Fig. 2.

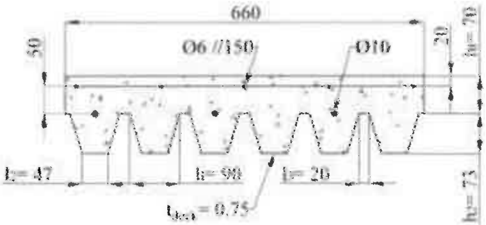

Fig. 2: Profile of the tested slab: dimensions in millimetres [4]

The specimen had a clear span of 660 mm wide by 3200 mm long. Normal weight concrete was used and the moisture content amounted to 3.5% by weight. The initial bulk temperature was of 20 °C.

4. Numerical modelling

In this section, the methodology used to numerically determine the thermal effects of standard fire exposure on composite slabs is outlined. In this regard, the finite elements, thermal material properties, boundary conditions and convergence criterion are presented. Finally, a comparison between the numerical and experimental results is given for the validation of the thermal model.

4.1 Thermal model

The composite slab is meshed to solve a nonlinear transient thermal analysis, using a 3-D model from ANSYS. The finite element method (FEM) requires the solution of Eq. (7) in the domain and the definition of the boundary conditions in Eq. (8) on the exposed and unexposed surface of the slab.

$$\nabla\left(\lambda_{(T)} \cdot \nabla T\right) = \rho_{(T)} \cdot Cp_{(T)} \cdot \partial T / \partial t \tag{7}$$

$$\lambda_{(T)} \cdot \nabla T \cdot \vec{n} = \alpha_c \cdot \left(T_g - T\right) + \Phi \cdot \varepsilon_m \cdot \varepsilon_f \cdot \sigma \cdot \left(T_g^4 - T^4\right) \tag{8}$$

In the equations above, T represents the temperature of each material; $\rho_{(T)}$ is the specific mass; $Cp_{(T)}$ is the specific heat; $\lambda_{(T)}$ is the thermal conductivity; α_c is the convection coefficient. T_g represents the gas temperature of the fire compartment, using the standard fire ISO 834 applied on the bottom part of the slab; Φ is the view factor; ε_m is the emissivity of each material; ε_f represents the emissivity of the fire and σ represents the Stefan-Boltzmann constant.

The view factor (Φ) quantifies the geometric relation between the surface emitting radiation and the surface receiving radiation. The view factor of the lower flange of composite slabs (Φ_{low}) is given as 1. Owing to the obstruction to direct fire exposure caused by the ribs of the steel deck, the view factors of the web (Φ_{web}) and upper flange (Φ_{upper}) are smaller than one. These view factors can be calculated as function of the geometric parameters of the slab, as follows.

$$\Phi_{upper} = \left[\sqrt{h_2^2 + \left(l_3 + \frac{l_1 - l_2}{2}\right)^2} - \sqrt{h_2^2 + \left(\frac{l_1 - l_2}{2}\right)^2}\right] \Big/ l_3 \tag{9}$$

$$\Phi_{web} = \left[\sqrt{h_2^2 + \left(\frac{l_1 - l_2}{2}\right)^2} + \left(l_3 + l_1 - l_2\right) - \sqrt{h_2^2 + \left(l_3 + \frac{l_1 - l_2}{2}\right)^2}\right] \Big/ 2\sqrt{h_2^2 + \left(\frac{l_1 - l_2}{2}\right)^2} \tag{10}$$

The finite element mesh for the slab of the validation model is presented in Fig. 3.

Fig. 3: Finite element mesh (ANSYS)

A three-dimensional model of the slab is generated, which is composed by subdomains that correspond to the different materials: the concrete topping, steel deck, rebars and steel mesh. Perfect thermal contact between all the materials is considered.

The thermal properties of the materials are temperature dependent and vary according to the standards used for composite structures [8], steel structures [9] and concrete structures [10]. The thermal properties of carbon steel and concrete are presented in Fig. 4. Regarding the conductivity of concrete, the upper limit has been selected for the numerical simulations. The specific heat of concrete presents a peak value related to 3% of moisture content of concrete weight. The extrapolation method was used to update higher moisture contents.

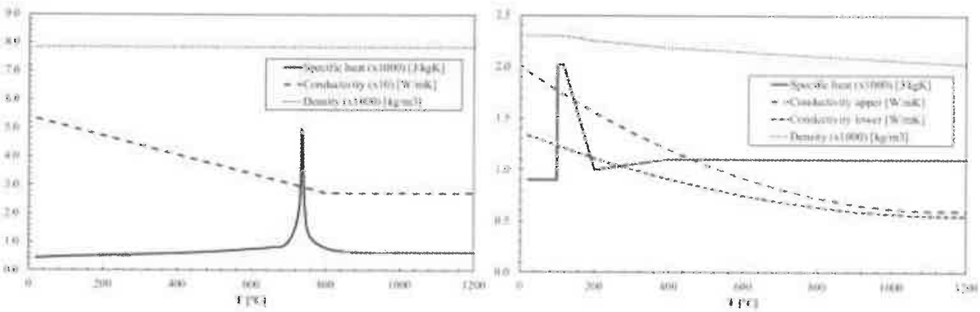

a) Carbon steel b) Concrete

Fig. 4: Thermal material properties

Three different finite elements are used: SHELL131, SOLID70 and LINK33. The SHELL131 element has four nodes with up to 32 degrees of freedom (temperature) per node, depending on the number of layers (one layer). This element presents linear interpolation functions in the plane of the element, using full Gauss integration method (2x2) and linear interpolation functions through the layer thickness (three Gauss points). The shell element is used to model the steel deck of the composite slab. The bottom temperature of shell element nodes is assumed to be equal to the temperature of solid element nodes, when both nodes are coincident. The SOLID70 element presents eight nodes with a single degree of freedom (temperature) at each node. Linear interpolation functions are used for this element and the full Gauss integration method is also applied (2x2x2). This finite element is used to model the concrete topping. The LINK33 element has two nodes with a single degree of freedom (temperature) per node. This uniaxial element presents linear interpolation functions and exact integration. The LINK33 element is used to model the anti-crack mesh and the rebars.

All the nodes are set with an initial condition for temperature of 20 °C. The exposed side is submitted to heat flux by convection and radiation, see Eq. (8), considering different values for view factors and the bulk temperature following the standard fire. The unexposed side is subjected to a convective heat flux, using a constant bulk temperature of 20 °C. The lower part of the steel deck is subjected to standard fire conditions using a convection coefficient of 25

W/m²K and an emissivity of fire equal to 1. A convective coefficient of 9 W/m²K is applied on the upper part of the composite slab in order to include the radiation effect [11].

The heat flow criterion is applied as convergence criterion, using a tolerance value of 10^{-3} and a minimum reference value of 10^{-6}.

4.2 Validation of the thermal model

Fig. 5 presents the temperature development (numerical and experimental) at different selected points, as well as the average and maximum temperatures on the unexposed side of the slab.

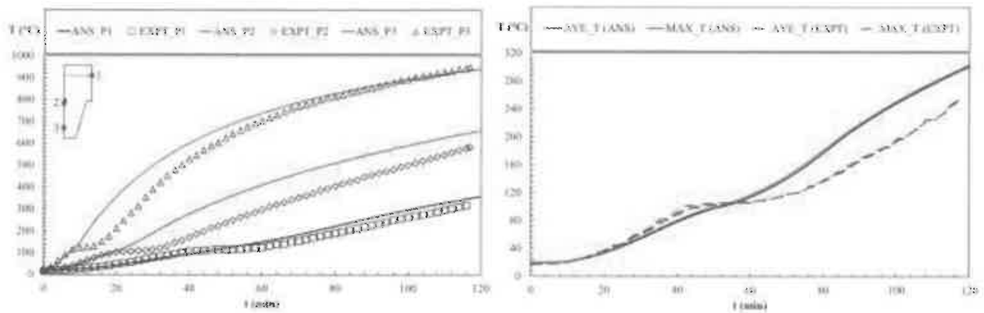

a) Selected points b) Unexposed side

Fig. 5: Numerical and experimental results – Points 1, 2 and 3 at distance 20, 74 and 123 mm from the top

With respect to the selected points, it can be observed that the temperature development on points 2 and 3 is quite similar between the experimental (EXPT) and the perfect contact model (ANS) in the first minutes of heating. After that, larger differences are observed, probably due to localized moisture concentrations in the experimental test, which are not considered in the numerical model. Additionally, this difference may be justified by the debonding of the steel deck from the concrete topping when the moisture evaporation starts (at about 100 °C), which increases the thermal resistance in this interface and is not considered in the thermal model. For point 1, a satisfactory agreement between the numerical and experimental results is obtained throughout the entire duration of the test.

Concerning the temperature development on the unexposed surface, the average and maximum temperature curves are very close to each other for both numerical and experimental results. Similarly to points 2 and 3, a good agreement between the numerical and experimental results is observed for both average and maximum temperatures until the first 60 minutes of heating.

5. Parametric study

A parametric study comprising slabs with commercial steel deck profiles has been conducted in order to analyse the influence of the steel components on the temperature of the parts of the steel deck (lower flange, web and upper flange) and the rebars as well. A total of 208 numerical simulations have been conducted in ANSYS considering perfect thermal contact between the materials and all the parameters are compared separately. Fig. 6 illustrates the geometry of the steel deck profiles.

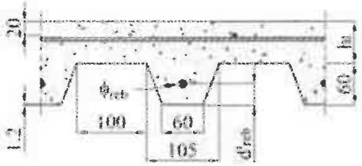

a) Slab 1: O Feliz H60

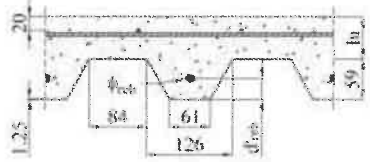

b) Slab 2: ArcelorMittal Polydeck 59.

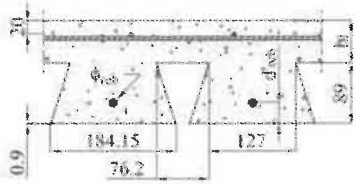

c) Slab 3: Vulcraft 3.5D Dovetail Formlok

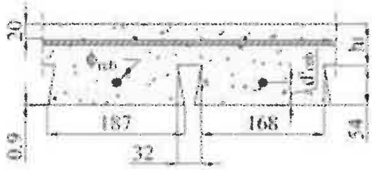

d) Slab 4: Lysaght Bondek

Fig. 6: Steel deck geometries for the parametric study: dimensions in millimetres

The ranges of selected parameters comprise commonly used values. The diameters and spacing of the anti-crack meshes have been determined from technical catalogues. A representative portion of 1 m by 1 m of each slab is selected to perform the thermal analyses considering standard fire conditions.

Fig. 7 presents the numerical results obtained in ANSYS (ANS) and the Eurocode 4 provisions (EC4) for the temperatures of the lower flange and the rebars, for the fire resistance class R60.

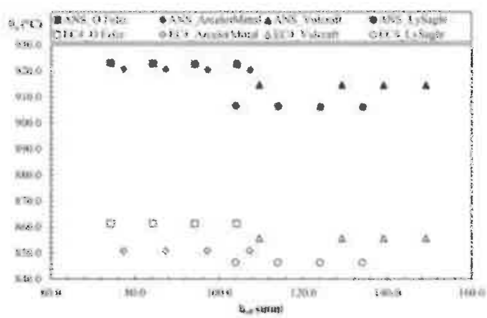

a) Temperature of the lower flange

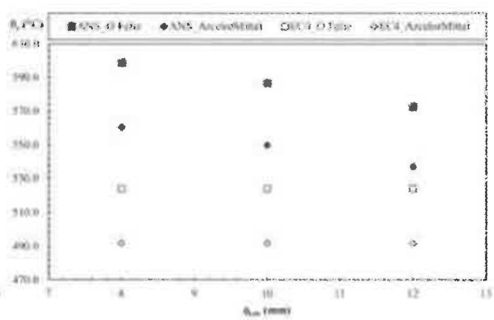

b) Temperature of the rebars (trapezoidal profiles)

Fig. 7: Comparison between the numerical results and EN 1994-1-2 provisions for the fire resistance class R60

According to the results above, it can be observed that the results from the Eurocode 4 – Part 1-2 for the temperature of the lower flange are considerably lower in comparison to the numerical results. This means that the calculation rules of the European standard are on the unsafe side. As stated by Ribeiro [12], the same is observed for the temperature of the web and the upper flange, as well as for the others fire resistance classes (R90 and R120).

With respect to the temperature of the rebars, it is observed that the temperatures obtained numerically are also higher than the Eurocode 4 results. Ribeiro [12] concluded that this occurs for most of the cases (81.5%) in a set of thermal analyses comprising slabs with trapezoidal and re-entrant profiles. In addition, it is noteworthy that the simplified calculation method of the standard does not include the effect of the diameter of the rebars on its temperature.

Based on the differences between the numerical results and the Eurocode 4 calculation rules for the temperature of the parts of the steel deck, new coefficients are proposed for composite slabs with NWC; see Eq. (1) and Table 3. The following table presents these coefficients for different classes of fire resistance (R).

Table 3: Proposed new coeff. for the temperature of the parts of the steel deck for slabs with NWC

Standard fire resistance	Part of the steel deck	b_0 (°C)	b_1 (°C mm)	b_2 (°C mm)	b_3 (°C)	b_4 (°C)
R60	Lower flange	*1015*	-1197	-2.32	86.4	*-147.5*
	Web	*725*	*600*	*-2.00*	537.7	*-356.0*
	Upper flange	*474*	*1300*	*-1.95*	1148.4	*-777.0*
R90	Lower flange	*939.5*	*95.0*	*1.00*	*93.0*	*-78.3*
	Web	*848.0*	*345.0*	-2.21	464.9	*-308.6*
	Upper flange	*641.5*	*854.0*	*-1.55*	*700.0*	*-315.0*
R120	Lower flange	*1106.0*	*-995.0*	*-1.55*	46.7	-82.8
	Web	*920.0*	*300.0*	-1.82	344.2	*-199.0*
	Upper flange	*764.0*	*660.0*	-1.67	592.6	*-271.0*

With respect to the temperature of the rebars in the rib, a new equation is also proposed, presenting a quadratic dependence between the diameter ϕ_{reb} (mm) and the temperature θ_s (°C) of the rebars. The new proposal is given in Eq. (11) and the proposed new coefficients for slabs with NWC are presented in Table 4.

$$\theta_s = c_0 + (c_1 \cdot u_3/h_2) + (c_2 \cdot z) + (c_3 \cdot A/L_r) + (c_4 \cdot \alpha) + (c_5 \cdot 1/l_3) + (c_6 \cdot \phi_{reb}^{\ 2}) + (c_7 \cdot \phi_{reb}) \quad (11)$$

Table 4: Proposed new coefficients for the determination of the temperatures of the rebars in the rib for slabs with NWC

Steel deck	Fire resistance	c_0 (°C)	c_1 (°C)	c_2 (°C mm$^{0.5}$)	c_3 (°C mm)	c_4 (°C/°)	c_5 (°C mm)	c_6 (°C/mm^2)	c_7 (°C/mm)
Trapezoidal	R60	*1294.90*	-250	-240	-5.01	1.04	-925	*-0.2425*	*-1.70*
	R90	*1406.81*	-256	-235	-5.30	1.39	-1267	*-0.1938*	*-1.6075*
	R120	*1407.65*	-238	-227	*-6.80*	*2.85*	-1326	*-0.7544*	*5.1688*
Re-entrant	R60	*1269.67*	-250	-240	-5.01	1.04	-925	*-0.160*	*-0.005*
	R90	*1363.63*	-256	-235	-5.30	1.39	-1267	*-0.1425*	*-0.215*
	R120	*1382.02*	-238	-227	-4.79	1.68	-1326	*-0.1413*	*-0.2875*

A comparison between this new proposal and the original version of EN 1994-1-2 was made for the composite slab under validation [4]. A reduction on the sagging moment resistance is verified according to this new proposal, see Table 5. The difference is in between 17 and 26%, being the calculation method from EN 1994-1-2 on the unsafe side.

Table 5: Comparison between the calculation method from EN 1994-1-2 and the new proposal for the sagging moment resistance

Fire Resistance	$M^{+}_{fi,r,Rd}$ (EN 1994-1-2) (N m)	$M^{+}_{fi,r,Rd}$ (New Proposal) (N m)	Difference (%)
R60	11256	8933	26
R90	8296	7071	17
R120	5519	4516	22

6. Conclusions

This paper presented a discussion around the results of 3-D thermal analyses performed in ANSYS for different composite slabs. The temperature of the steel components has been evaluated and compared to experimental results and the simplified calculation method of Eurocode 4. The numerical model has been successfully validated with the experimental fire test.

For the experimental results, a plateau at about 100 °C (due to moisture evaporation) should be highlighted, consisting of a decrease in the rate of temperature increase. The results of the numerical simulations do not present this pronounced plateau, probably because localized moisture concentrations in the tests were higher than the uniform moisture content introduced in the thermal model.

With respect to the results obtained through the calculation rules from EN 1994-1-2, the temperature of the steel components was on the unsafe side for most of the analyses of the parametric study, which can lead to the unsafe design of composite structures under fire.

Based on the numerical results, new calculation formulae have been proposed for the determination of the temperature of the steel components of the composite slab (parts of the steel deck and rebars). These new methods present good agreement with numerical results and consider parameters which are not included in the current calculation rules of the European standard. According to this new proposal, the fire resistance is reduced in comparison to the calculation method of the current version of Eurocode 4 – Part 1-2.

References

[1] International Standard ISO 834, "Fire-resistance tests - Elements of building construction. Part 1: General requirements" 1999.

[2] J. Jiang, A. Pintar, J. M. Weigand, J. A. Main, and F. Sadek, "Improved calculation method for insulation-based fire resistance of composite slabs," *Fire Safety Journal*, vol. 105, pp. 144–153, Mar. 2019.

[3] European Convention for Constructional Steelwork - Committee T3 - Fire Safety of Steel Structures, "Calculation of the fire resistance of composite concrete slabs with profiled steel sheet exposed to the standard fire," *ECCS: Publication 32*, p. 48, 1983.

[4] A. F. Hamerlinck, "The behaviour of fire-exposed composite steel/concrete slabs," Eindhoven University of Technology, 1991.

[5] C. Both, "The fire resistance of composite steel-concrete slabs," Technical University of Delft, 1998.

[6] L. Lim and C. Wade, "Experimental fire tests of two-way concrete slabs," Christchurch, 2002.

[7] S. Guo and C. G. Bailey, "Experimental behaviour of composite slabs during the heating and cooling fire stages," *Engineering Structures*, vol. 33, pp. 563–571, 2011.

[8] CEN- European Committee for Standardization, *EN 1994-1-2: Design of composite steel and concrete structures. Part 1-2: General rules - Structural fire design*. Brussels: CEN-European Committee for Standardization, 2005.

[9] CEN- European Committee for Standardization, *EN 1993-1-2: Design of steel structures - Part 1-2: General rules - Structural fire design Eurocode*. Brussels: CEN - European Committee for Standardization, 2005.

[10] CEN- European Committee for Standardization, *EN 1992-1-2: Design of concrete structures - Part 1-2: General rules - Structural fire design*, vol. EN 1992. Brussels: CEN - European Committee for Standardization, 2004.

[11] CEN- European Committee for Standardization, *EN 1991-1-2, Eurocode 1: Actions on structures – Part 1-2: General actions – Actions on structures exposed to fire*. Brussels: CEN- European Committee for Standardization, 2002.

[12] F. F. Ribeiro, "Numerical simulation of composite slabs with steel deck under fire conditions" (Master's thesis), Polytechnic Institute of Bragança, 2019.

cmm
ASSOCIAÇÃO PORTUGUESA DE
CONSTRUÇÃO METÁLICA E MISTA

Secretariado da CMM
Business Center Leonardo Da Vinci, lt.3 iParque,
3040-540 Antanhol, Coimbra, Portugal

cmm@cmm.pt
www.cmm.pt